PHYSICAL REVIEW B **90**, 041410(R) (2014)

Tunable switching dynamics of a single Si dopant in GaAs(110)

E. P. Smakman,* P. L. J. Helgers, J. Verheyen, and P. M. Koenraad
Faculty of Applied Physics, Eindhoven University of Technology, Eindhoven, The Netherlands

R. Möller
Faculty of Physics and Center for Nanointegration, University of Duisburg-Essen, Duisburg, Germany
(Received 13 February 2014; revised manuscript received 17 June 2014; published 22 July 2014)

The dynamic behavior of single bistable Si dopants in the GaAs (110) surface, which switch between a positive and a negative charge configuration, was investigated using a scanning tunneling microscope (STM) and noise analysis electronics. The dopant atom switching frequency shows a clear dependence on the bias voltage and tunneling current, because these parameters influence the escape and capture processes of electrons. Our physical model for these processes, taking into account the relevant tunneling barriers, matches well with the experimental data. By choosing the appropriate tunneling conditions, we show that a single dopant can be employed as a memory element. The STM tip serves both as an electrical gate to write and as a probe to read the information stored on a single Si atom.

DOI: 10.1103/PhysRevB.90.041410 PACS number(s): 73.20.Hb, 66.35.+a, 85.35.−p

Moore's law [1] describes the tremendous downscaling of the size of a transistor in the past decades. An equal trend has affected other electronic components such as, for instance, a memory cell. Reducing the size of current flash memory further could potentially decrease the energy needed for operation and increase the read and write speed. It is an ultimate dream to realize charge-based electronic functionality such as nonvolatile memory operations on a single atom that is locked into place in a semiconductor host [2]. Several examples of atomic-scale charge-based electronic device functionality have been demonstrated recently. For instance, on atomically flat surfaces, chains of atoms [3,4] and dangling bonds [5,6] were constructed that can be employed in logic operations. In other studies, charge manipulation on single dopants is reported that allows the tuning of the local electronic transport through transistor devices [7,8]. Furthermore, purely mechanical bistable atomic-scale systems have been demonstrated in the form of molecule cascades [9], buckled dimers at the Si (100) surface [10], and atomic break-junction structures [11]. In this Rapid Communication, we investigate the dynamics of a single bistable Si dopant in the GaAs (110) surface with scanning tunneling microscopy (STM) and connect the switching behavior with a physical model to the relevant tunneling barriers in the system. Furthermore, we show how a single Si dopant atom has been successfully used as a memory cell on which the information can be stored $\geqslant$25 s, albeit with switching times on the second time scale at $T = 5$ K. We suggest that there is no fundamental objection to transfer this approach to a device in the bulk because similar bistable behavior is well known for the same Si dopant embedded in bulk AlGaAs, known as the DX^- center [12].

GaAs n-type wafers doped with a Si concentration of $\sim 2 \times 10^{18}$ cm^{-3} were used in the experiments. To obtain atomically flat and clean (110) surfaces, the samples were cleaved in ultrahigh vacuum (UHV) under a pressure of $\leqslant 2 \times 10^{-11}$ mbar. The measurements were performed in an Omicron low-temperature scanning tunneling microscope (LT-STM) operated at $T = 5$ and 77 K. Polycrystalline W wires were electrochemically etched to obtain tips with an atomically sharp apex. Tip heating and Ar sputtering were done under UHV conditions for improved stability.

Si in GaAs is a dopant that is well studied by STM [13,14]. Recently, bistable behavior of Si atoms in the (110) surface layer of GaAs was observed during scanning with a STM tip [15,16]. Only and all the Si dopants in the surface layer exhibit this behavior; the dopants below the surface do not. Figure 1 illustrates this bistability with STM topographic images of the same Si dopant. The bright contrast, stable at relatively high bias voltage, resembles a positively charged Si donor coordinated on a Ga site in the lattice, which is relaxed inwards with respect to the surface, denoted as Si_d^+. A clear ionization disk can be observed around the dopant, which corresponds to the boundary between the neutral and positive charge state of the Si atom. The ionization occurs through the local presence of the tip due to tip induced band bending (TIBB) [17,18]. Density functional theory (DFT) calculations confirm that the dark contrast, stable at relatively low bias voltage, corresponds to a negatively charged Si, denoted as Si_i^- [19]. It has moved slightly in the lattice, from the original relaxed Ga site to a position located more outwards with respect to the surface. Si_i^- is energetically the most favorable configuration in the (110) surface of GaAs. Both configurations are metastable, meaning that an energy barrier E_{bar} has to be overcome to switch from one state to the other [12,20]. If the TIBB is large, electrons from the dopant can escape into the conduction band of the semiconductor host, resulting in Si_d^+. The opposite process of electron capture depends on the current injected by the tip. If the TIBB is small, captured electrons remain bound to the dopant atom, resulting in Si_i^-. Continuous switching occurs when both processes are active. Although in principle the neutral charge state of the donorlike configuration is stable at low temperature, in the experiments presented in this work the TIBB of the STM tip located directly on top of a bistable Si always resulted in either the positive or the negative charge configuration.

*e.p.smakman@tue.nl

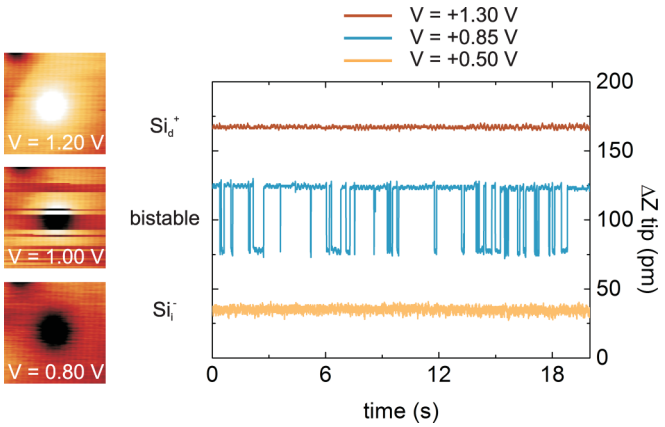

FIG. 1. (Color online) Left: 8×8 nm^2 STM topography images of a single bistable Si atom in the GaAs (110) surface, where the fast scan direction is left to right and the slow scan direction is bottom to top. $I = 70$ pA and $T = 5$ K. Right: STM tip height traces recorded in time, offset from each other for clarity. The top brown line corresponds to a stable Si_d^+ and the bottom orange line to a stable Si_i^-. The middle blue line shows the switching behavior in time as random telegraph noise. $I = 75$ pA and $T = 77$ K.

In several experiments described in this work, the Z position of the STM tip was recorded in time, giving information about the charge state of a bistable Si atom. These measurements were conducted while the tip was in tunneling contact in constant current mode, but was restricted to a single point exactly on top of a bistable Si. This measurement configuration allows the recording of random telegraph noise of the switching when specific tunneling conditions are applied (see Fig. 1). The random telegraph signal noise data were taken at low temperature to limit both the horizontal and lateral drift of the tip and sample. The distance between tip and sample, which can only be estimated, is in the order of 1 nm. However, the tip height ΔZ is the exact distance with respect to a fixed reference level determined by the piezomotors of the STM. For every combination of bias voltage and tunneling current, the tip height changes accordingly. Therefore, in order to determine the Si charge state, a reference measurement on the surrounding GaAs material is needed. We recorded two-dimensional (2D) topographic images to obtain the charge state of the Si atom for every applied tunneling condition. This information is then used to determine the charge state when the tip is restricted to a single point. In the figure, the middle blue line shows bistable behavior of a dopant at a critical bias voltage of $V = +0.85$ V. The switching frequency at these conditions is about 1 Hz. Si_d^+ appears as an elevation in the surface corresponding to a retracted tip, while Si_i^- shows up as a depression corresponding to an extended tip. The difference in tip-sample distance between Si_d^+ and Si_i^- is in the order of 50 pm, which is well above the Z-noise level of the STM of about 5 pm. The top brown line is taken on top of the same bistable Si atom and shows a stable charge level corresponding to Si_d^+. Similarly, the bottom orange line represents Si_i^-.

In Fig. 2, various random telegraph noise measurements on single bistable Si dopants are presented that reveal the dynamic behavior of the switching process. For these measurements, analog electronics analyzing the tunneling current

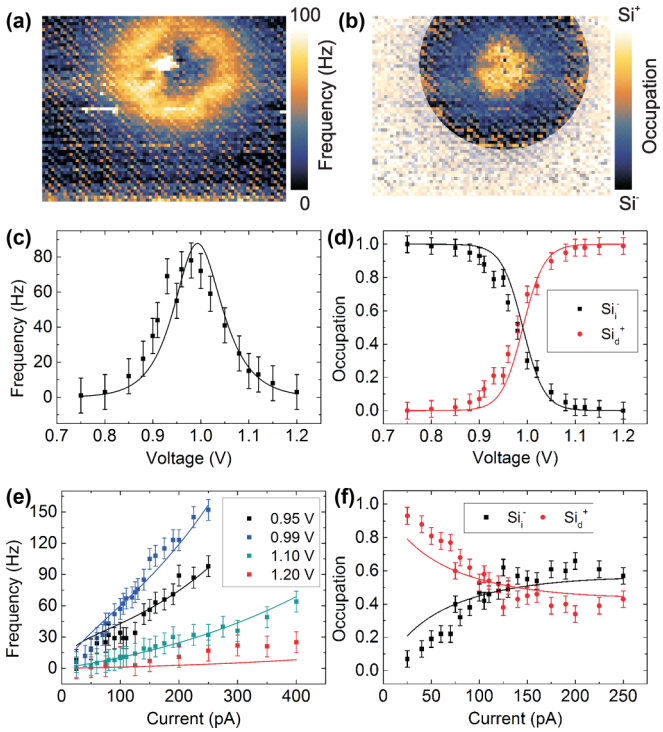

FIG. 2. (Color online) 2D maps of 8×6 nm^2, taken at $V = +0.75$ V and $I = 500$ pA, showing the spatial distribution of (a) the frequency and (b) the occupation of the positive and negative charge state, the latter within a circle of confidence. Switching frequency recorded at the center of the bistable dopant as a function of (c) bias voltage taken at $I = 150$ pA and (e) average tunneling current. Occupation of states as a function of (d) bias voltage taken at $T = 150$ pA and (f) average tunneling current taken at $V = +0.99$ V. Dots are the measurements, error bars originate from the noise in STM height data, and lines are fits of the data with Eq. (3). Measurements were obtained at $T = 5$ K.

were combined with the STM in order to evaluate the switching frequency and the occupation of the two charge states [21,22].

In Figs. 2(a) and 2(b) 2D maps on and around a bistable Si are depicted that represent the switching frequency and occupation of the positive charge state, respectively. Depending on the exact location of the tip, the TIBB and current density at the location of the Si atom vary and thereby influence the dynamics of the dopant. When the tip is exactly on top of the Si, the positive charge state is dominant and the switching frequency is low. With the tip farther away, the negative charge state becomes more and more favored and the switching frequency increases. When the tip is even farther away, the negative charge state is dominant and the frequency drops again.

Measurements visible in Figs. 2(c)–2(f) were taken directly on top of another bistable Si for varying bias voltage and tunneling current, with the tip restricted to a single point. In this case, analysis was performed directly on the STM topographic height data, to appropriately take into account the changing height difference between the two charge states when varying the tunneling conditions. The observed switching frequency in Fig. 2(c) exhibits a maximum value around a critical bias voltage. This maximum coincides with an occupation of 0.50 for both configurations, visible in Fig. 2(d), indicating this

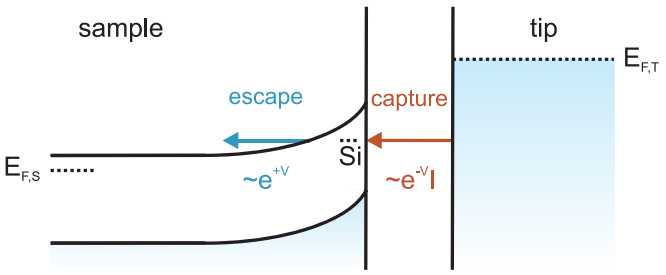

FIG. 3. (Color online) Energy diagram emphasizing the important physical processes involved in the switching.

is the point where escape and capture processes of electrons are of equal importance. Below the critical voltage, the escape rate of electrons is dominating, because that process is limiting the switching. Similarly, above the critical voltage, the capture rate of electrons is dominating. In Fig. 2(e) the switching frequency is depicted as a function of tunneling current for a few different bias voltages. Over the whole voltage range, the frequency scales roughly linear with the tunneling current. In Fig. 2(f), the occupation of the two charge states is shown on the same current scale. In this case, the occupation of the negative charge state increases gradually with the tunneling current. Both effects as a function of current occur because more electrons are available for capture.

To model the dynamic behavior of the charge switching, the escape and capture processes can be described independently. The average time to switch from Si_i^- to Si_d^+ and back is $\langle\tau\rangle = \langle\tau_-\rangle + \langle\tau_+\rangle$, where $\langle\tau_-\rangle$ is the average time in Si_i^- and $\langle\tau_+\rangle$ the average time in Si_d^+. The physical processes involved in the capture and escape are summarized in Fig. 3.

If the bias voltage V is increased at constant tunneling current I, or I is decreased at constant V, the vacuum barrier between the tip and the bistable dopant increases. This makes it harder for electrons with the same energy as the Si state to tunnel from the tip to the dopant level and be captured. We assume an exponential relation between the tunneling probability and V and I. Additionally, we expect that the switching is limited by the electron that brings the dopant from Si_d^+ to the neutral charge state at a shifted lattice position. The subsequent process of capturing another electron is fast and efficient. Therefore the capture process depends linearly on the tunneling current, which results in the following relation for the capture rate $f_{+|-}$:

$$f_{+|-} = \langle\tau_-\rangle^{-1} = a_1 e^{-\frac{V}{b_1}+\frac{I}{c_1}} I, \tag{1}$$

where a_1, b_1, and c_1 are scaling coefficients.

For the opposite process of ionization a similar relation exists for the escape rate $f_{-|+}$, if we consider that it is easier for electrons to escape the dopant with increasing TIBB. This is included as an exponential growth factor in the model, because the width of the tunneling barrier in the sample between the Si state and the GaAs conduction band decreases with larger V, as well as with larger I. This results in

$$f_{-|+} = \langle\tau_+\rangle^{-1} = a_2 e^{+\frac{V}{b_2}+\frac{I}{c_2}}, \tag{2}$$

where a_2, b_2, and c_2 are scaling coefficients.

The switching frequency f, the negative charge state occupation n_-, and the positive charge state occupation n_+ that are observed in the measurement are expressed as

$$\begin{aligned} f &= \langle\tau\rangle^{-1} = \frac{f_{+|-} f_{-|+}}{f_{+|-} + f_{-|+}}, \\ n_- &= f_{-|+}^{-1} f, \\ n_+ &= f_{+|-}^{-1} f. \end{aligned} \tag{3}$$

The data recorded on a single dopant shown in Figs. 2(c)–2(f) were fitted with the physical model using Eq. (3). The following fitting procedure was used. The parameters b_1 and b_2 were estimated from the f vs V data. Using this as input, the f vs I data sets yielded the starting point for parameters c_1 and c_2. The occupation data then served as a further optimization and gave the range for parameters a_1 and a_2. In the final step, the fits on the full data set were optimized to find the best global match. We find $a_1 = 1.3$ GHz/pA, $a_2 = 4.7$ μHz, $b_1 = 47$ mV, $b_2 = 42$ mV, $c_1 = 0.60$ nA, and $c_2 = 0.20$ nA. The large difference in order of magnitude between a_1 and a_2 is there because the offset for the frequency distribution maximum in terms of V is part of the prefactors. Moreover, the exponents contain both positive and negative contributions, further enhancing the difference between a_1 and a_2. The fits demonstrate that both the voltage and current dependence of the model are in good agreement with the experimental data. The switching frequencies in the order of $\sim$100 Hz observed here are orders of magnitude lower than, for example, the $\sim 10^6$ Hz seen in the hopping of CO molecules on Cu (111), described in Ref. [9]. Moreover, tunneling currents of $\sim$200 pA used in the experiments correspond to $\sim 10^9$ electrons s^{-1}, which implies that at $T = 5$ K only 1 in 10^7 electrons is captured on the dopant atom when the tip is located directly on top.

The fit parameters are related to the tunneling process and its relevant tunneling barriers and therefore do not give quantitative information about the switching mechanism itself. However, from $I(Z)$ data, directly available from the measurements presented in Figs. 2(c)–2(f), a rough measure for the TIBB at the surface can be determined [23,24]. Employing iterative calculations of the Poisson equation and the tip work function using the method developed by Feenstra in Ref. [25], we determine the flatband condition to be $V_{FB} = -0.9 \pm 0.7$ V. The switching frequency maximum at $V = +0.98$ V results in a TIBB at the surface of $E_{BB} = 0.4 \pm 0.2$ eV. Both values confirm that indeed the studied system experiences positive band bending for all experimentally applied bias voltages, as is assumed in this work. The onset of the switching starts approximately around $V = +0.80$ V, at a TIBB of $E_{BB} = 0.3 \pm 0.1$ eV. The latter value is a measure for the binding energy of the Si_i^- configuration, because then the dopant level at the surface aligns with the conduction band edge in the bulk, allowing the escape of electrons. This observation corresponds well to the DFT calculations that predict that this state is a deep trap [19,26].

Through understanding of the dynamic behavior of the Si dopant, we can choose the tunneling conditions such that it can be employed for demonstrating memory operations on a single atom. The Si charge state is nonvolatile at low

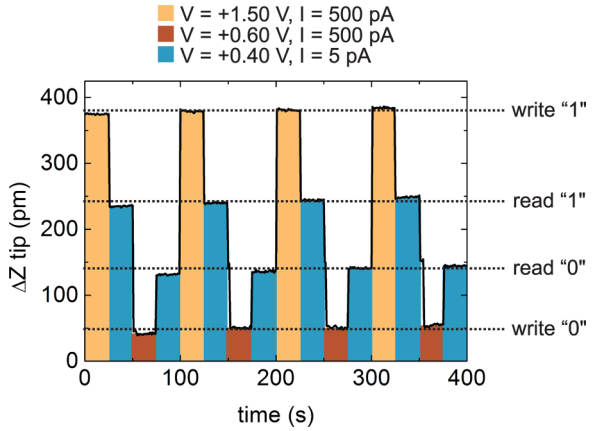

FIG. 4. (Color online) The solid line is a measurement of the STM tip height in time showing the repeated operation on an Si atom acting as a memory element. The colors indicate different applied tunneling conditions and the dotted lines the resulting STM tip height levels. $T = 5$ K.

temperatures, which enables the storage of information [16]. For memory operation, three separate conditions need to be distinguished: (a) setting the system to Si_i^-, (b) setting it to Si_d^+, and (c) detecting the charge state. The two states can be set by choosing the bias voltage either relatively low or high, respectively. If the energy eV of the STM-injected electrons is lower than the energy barrier between the two configurations, the switching can no longer take place, which allows the determination of the charge state without the STM tip affecting it.

Figure 4 shows experimental results where the bistability of Si was used for performing memory operations. In this measurement, the STM tip was restricted on top of a single bistable Si dopant in constant current mode and the height of the tip was recorded. To set a different tunneling condition, the measurement was paused several seconds, after which the voltage and current were adjusted before the measurement continued. The current was changed to lower the chance of a switch during the readout phase, which means it was adjusted before changing the voltage to the readout setting and after changing the voltage to a write setting. The data points were taken at 1 kHz and every tunneling condition was set for 25 s. Three different tunneling conditions were applied in sequence and the recorded pattern was repeated four times to show the reproducibility. We demonstrate the single atom memory is stable for at least 25 s.

A relatively high bias voltage of $V = +1.50$ V and a high tunneling current of $I = 500$ pA favor the occupation of Si_d^+, because the electrons on the Si atom can tunnel into the conduction band due to the large enough TIBB. We see no noticeable delay time in the change from negative to positive charge. In the figure we observe this "write (1)" condition as the regions with the largest tip height. The high voltage setting is the most flexible and stable of the three read and write conditions and works from about $V = +1.25$ V up to higher values. Below that the Si atom becomes bistable.

At an intermediate bias voltage of $V = +0.60$ V the Si atom switches to the negative charge state. Here the switching time is on average 1 s, which can be seen in the data as a plateau at a larger tip height level for a short time, after which the atom switches to Si_i^-. The relatively long delay time for the "write (0)" condition is very different from that of the opposite process. For writing a (1), electrons need to escape into the conduction band, and at high TIBB this occurs very quickly. For writing a (0), two electrons supplied by the STM tip need to be captured by the Si atom and the chance for this is apparently small. The switching frequency increases with increasing tunneling current, but in this experiment $I = 500$ pA was the highest current we could apply without crashing the tip into the surface. The voltage condition corresponding to electron capture is quite critical, because a too high voltage leads to random switching and a lower voltage considerably extends the write delay.

A low bias voltage of $V = +0.40$ V does not influence the system and allows a "readout" of the Si charge state. To test for any hysteresis in the system, we applied several high and intermediate voltages in sequence, followed by a readout at low voltage. The readout always depended on the last write step only. The low current of $I = 5$ pA was chosen to stabilize the readout condition. A higher voltage increases the chance at writing a (0) and a lower voltage leads to more tip instability because it is tunneling closer to the band gap.

We postulate that the Coulomb interaction between bistable Si atoms can be used to build logic operators [27]. For this it is essential that the Si dopants can be positioned with atomic-scale precision in the surface. Several methods have already been employed in other studies to embed dopants with high spatial accuracy [7,28]. A charged Si dopant changes its surrounding potential landscape and therefore influences another Si dopant that is close enough. For instance, if a Si is negatively charged, the local upward band bending will make it easier for neighboring Si to switch to the positive charge state. In this approach we expect that one can construct logic gates with multiple bistable Si atoms. Control over the charge state at the surface can be achieved by local gates and scanning probe techniques such as STM [17,29] and atomic force microscopy (AFM) [3,30].

The application of embedded dopants as functional elements in a host material allows device operation outside UHV. The well-known bistable DX^- center in bulk [12], associated with, for instance, a single Si dopant in AlGaAs, can be utilized in a similar manner as the presently studied Si in the GaAs surface. If the precise location of Si atoms embedded in bulk AlGaAs can be controlled or known, local nanoscale contacts and gates can be used to manipulate and probe a single Si DX^- center. This approach should thus allow for the creation of atomic-size charge-based devices, for instance, memory cells or tunnel field-effect transistors (TFETs) [31]. Such devices can operate outside of UHV conditions and enable integration into more advanced electronic structures. Important prerequisites for real devices are the stability of the charge configurations at room temperature as well as the ability to write and readout at frequencies much higher than the dynamic range studied in this work.

In conclusion, the experiments and modeling of the switching dynamics of bistable Si atoms in the GaAs (110) surface reveal that electron escape and capture processes depend strongly on the applied tunneling conditions. We have demonstrated memory operations on a bistable Si dopant,

where the STM tip acts as a gate for reading and writing the information.

The funding for this work was provided by FOM (Grant No. 09NSE06). We thank J. van Bree for valuable discussions.

[1] G. E. Moore, Electronics **38**, 114 (1965).
[2] P. M. Koenraad and M. E. Flatté, Nat. Mater. **10**, 91 (2011).
[3] J. Repp, G. Meyer, F. E. Olsson, and M. Persson, Science **305**, 493 (2004).
[4] J. Yang, S. C. Erwin, K. Kanisawa, C. Nacci, and S. Fölsch, Nano Lett. **11**, 2486 (2011).
[5] M. B. Haider, J. L. Pitters, G. A. DiLabio, L. Livadaru, J. Y. Mutus, and R. A. Wolkow, Phys. Rev. Lett. **102**, 046805 (2009).
[6] S. R. Schofield, P. Studer, C. F. Hirjibehedin, N. J. Curson, G. Aeppli, and D. R. Bowler, Nat. Commun. **4**, 1649 (2013).
[7] M. Fuechsle, J. Miwa, S. Mahapatra, H. Ryu, S. Lee, O. Warschkow, L. C. L. Hollenberg, G. Klimeck, and M. Y. Simmons, Nat. Nanotechnol. **7**, 242 (2012).
[8] H. Zheng, A. Weismann, and R. Berndt, Nat. Commun. **5**, 2992 (2014).
[9] A. J. Heinrich, C. P. Lutz, J. A. Gupta, and D. M. Eigler, Science **298**, 1381 (2002).
[10] A. Sweetman, S. Jarvis, R. Danza, J. Bamidele, L. Kantorovich, and P. Moriarty, Phys. Rev. B **84**, 085426 (2011).
[11] C. Schirm, M. Matt, F. Pauly, J. C. Cuevas, P. Niebala, and E. Scheer, Nat. Nanotechnol. **8**, 645 (2013).
[12] P. M. Mooney, Semicond. Sci. Technol. **6**, B1 (1991).
[13] J. F. Zheng, X. Liu, N. Newman, E. R. Weber, D. F. Ogletree, and M. Salmeron, Phys. Rev. Lett. **72**, 1490 (1994).
[14] R. M. Feenstra, G. Meyer, F. Moresco, and K. H. Rieder, Phys. Rev. B **66**, 165204 (2002).
[15] J. K. Garleff, A. P. Wijnheijmer, C. N. Van Den Enden, and P. M. Koenraad, Phys. Rev. B **84**, 075459 (2011).
[16] E. P. Smakman, J. van Bree, and P. M. Koenraad, Phys. Rev. B **87**, 085414 (2013).
[17] K. Teichmann, M. Wenderoth, S. Loth, R. G. Ulbrich, J. K. Garleff, A. P. Wijnheijmer, and P. M. Koenraad, Phys. Rev. Lett. **101**, 076103 (2008).
[18] A. P. Wijnheijmer, J. K. Garleff, K. Teichmann, M. Wenderoth, S. Loth, and P. M. Koenraad, Phys. Rev. B **84**, 125310 (2011).
[19] Z. Yi, Y. Ma, and M. Rohlfing, J. Phys. Chem. C **115**, 23455 (2011).
[20] D. J. Chadi and K. J. Chang, Phys. Rev. B **39**, 10063 (1989).
[21] J. Schaffert, M. C. Cottin, A. Sonntag, H. Karacuban, C. A. Bobisch, N. Lorente, J.-P. Gauyacq, and R. Möller, Nat. Mater. **12**, 223 (2012).
[22] J. Schaffert, M. C. Cottin, A. Sonntag, H. Karacuban, D. Utzat, C. A. Bobisch, and R. Möller, Rev. Sci. Instrum. **84**, 043702 (2013).
[23] S. Loth, M. Wenderoth, R. G. Ulbrich, S. Malzer, and G. H. Döhler, Phys. Rev. B **76**, 235318 (2007).
[24] A. P. Wijnheijmer, J. K. Garleff, M. A. Van Der Heijden, and P. M. Koenraad, J. Vac. Sci. Technol. B **28**, 1086 (2010).
[25] R. M. Feenstra, J. Vac. Sci. Technol. B **21**, 2080 (2003).
[26] J. Wang, T. A. Arias, J. D. Joannopoulos, G. W. Turner, and O. L. Alerhand, Phys. Rev. B **47**, 10326 (1993).
[27] C. S. Lent and P. D. Tougaw, Proc. IEEE **85**, 541 (1997).
[28] D. Kitchen, A. Richardella, J.-M. Tang, M. E. Flatté, and A. Yazdani, Nature (London) **442**, 436 (2006).
[29] D. H. Lee and J. A. Gupta, Nano Lett. **11**, 2004 (2011).
[30] L. Gross, F. Mohn, P. Liljeroth, J. Repp, F. J. Giessibl, and G. Meyer, Science **324**, 1428 (2009).
[31] W. M. Reddick and G. A. J. Amaratunga, Appl. Phys. Lett. **67**, 494 (1995).